

Geophysical Research Letters®



RESEARCH LETTER

10.1029/2022GL098944

Key Points:

- Novel framework for identifying and quantifying groundwater flow through buried paleo-channels
- Heterogeneous hydraulic conductivity fields were identified based on spatially varying, preferred anisotropy-constrained inversion
- The fraction of infiltrating stream water in the aquifer and stream-aquifer exchange fluxes best inform the paleo-channel

Supporting Information:

Supporting Information may be found in the online version of this article.

Correspondence to:

O. S. Schilling,
oliver.schilling@unibas.ch

Citation:

Schilling, O. S., Partington, D. J., Doherty, J., Kipfer, R., Hunkeler, D., & Brunner, P. (2022). Buried paleo-channel detection with a groundwater model, tracer-based observations, and spatially varying, preferred anisotropy pilot point calibration. *Geophysical Research Letters*, 49, e2022GL098944. <https://doi.org/10.1029/2022GL098944>

Received 31 MAR 2022

Accepted 18 JUN 2022

Author Contributions:

Conceptualization: O. S. Schilling, J. Doherty

Data curation: O. S. Schilling

Formal analysis: O. S. Schilling, D. J. Partington

Funding acquisition: P. Brunner

Investigation: O. S. Schilling

Methodology: O. S. Schilling, D. J. Partington, J. Doherty, P. Brunner





Resources: R. Kipfer, D. Hunkeler

Supervision: P. Brunner

Validation: O. S. Schilling

Visualization: O. S. Schilling

Buried Paleo-Channel Detection With a Groundwater Model, Tracer-Based Observations, and Spatially Varying, Preferred Anisotropy Pilot Point Calibration

O. S. Schilling^{1,2,3} , D. J. Partington⁴ , J. Doherty^{4,5}, R. Kipfer^{3,6,7}, D. Hunkeler¹ , and P. Brunner¹ 

¹Centre for Hydrogeology and Geothermics (CHYN), University of Neuchâtel, Neuchâtel, Switzerland, ²Hydrogeology, Department of Environmental Sciences, University of Basel, Basel, Switzerland, ³Eawag, Swiss Federal Institute of Aquatic Science and Technology, Dübendorf, Switzerland, ⁴National Centre for Groundwater Research & Training (NCGRT), College of Science & Engineering, Flinders University, Adelaide, SA, Australia, ⁵Watermark Numerical Computing, Corinda, QLD, Australia, ⁶Institute of Biogeochemistry and Pollutant Dynamics, Swiss Federal Institute of Technology (ETH), Zürich, Switzerland, ⁷Institute of Geochemistry and Petrology, ETH Zürich, Zürich, Switzerland

Abstract Alluvial sand and gravel (ASG) aquifers are highly heterogeneous and exhibit strong, spatially variable anisotropy, often interspersed by buried paleo-channels of increased hydraulic conductivity. Groundwater flow and solute transport is often characterized by preferential flow caused by anisotropic properties in ASG aquifers. Connected ASG subsurface structures such as buried paleo-channels, however, are difficult to reproduce with commonly used techniques, and anisotropy is rarely considered in applied groundwater models. To ease the notoriously difficult problem of how to consider anisotropy, we propose a novel modeling framework based on calibration of an integrated surface-subsurface hydrological model via spatially varying, preferred anisotropy pilot point inversion. The inversion leverages hydraulic and tracer-based observations representing multiple spatial and temporal scales. We demonstrate the applicability of the framework on a real-world ASG site used for drinking water production, and we quantify the information content of observations to identify connected paleo-channels and provide guidance for optimal field-data acquisition.

Plain Language Summary Mountainous river corridors are used worldwide for drinking water production, as they represent a relatively safe and sustainable source of drinking water. The valley-fill of mountainous river corridors is a result of millennia of fluvio-glacial erosion and deposition via braided river systems and consists primarily of poorly sorted sand and gravel. Groundwater flow and solute transport through such alluvial sand and gravel (ASG) aquifers is characterized by preferential flow paths caused by formerly active, now buried meanders (i.e., paleo-channels). The identification of paleo-channels in ASG aquifers is crucial for safe drinking water production, but they are notoriously difficult to identify with the commonly used techniques. We propose a new modeling framework based on the calibration of an integrated surface-subsurface hydrological model via spatially varying, preferred anisotropy pilot point inversion using both hydraulic and tracer observations. The new modeling framework is more efficient than other approaches to model flow through complex ASG aquifers and doesn't require precise prior knowledge of the location of paleo-channels. The applicability and robustness of the framework is demonstrated on an ASG drinking water wellfield located in the Swiss Alps.

1. Introduction

Mountainous river corridors are used worldwide for drinking water production, as they represent a relatively safe and sustainable source of water. The valley-fill of mountainous river corridors is formed by millennia of fluvio-glacial erosion and deposition via braided rivers and streams, and consists primarily of poorly sorted gravel, cobbles and sand (Bridge & Demicco, 2008). As opposed to aquifer types in which heterogeneity originates from intersecting of various sediments, conduits or fractures, the heterogeneity of alluvial sand and gravel (ASG) aquifers arises from the consecutive layering of variably arranged streambed and floodplain sediments (Bayer et al., 2011; Hoehn, 2002; Huggenberger et al., 2013; Limaye & Lamb, 2014). ASG aquifers are highly conductive for groundwater (GW) flow and characterized by strong, spatially variable horizontal anisotropy, which results from the strong spatial correlation and extended connectivity of hydraulic properties in the downvalley

© 2022 The Authors.

This is an open access article under the terms of the [Creative Commons Attribution-NonCommercial License](https://creativecommons.org/licenses/by-nc/4.0/), which permits use, distribution and reproduction in any medium, provided the original work is properly cited and is not used for commercial purposes.

Writing – original draft: O. S. Schilling
Writing – review & editing: O. S. Schilling, R. Kipfer, P. Brunner

direction (Bridge & Demicco, 2008; Jussel et al., 1994a; Siegenthaler & Huggenberger, 1993). The principal discharge regime responsible for the formation of the majority of ASG aquifers in lower-sloping, mountainous regions is characterized by the repeated alternation of extended *dynamic equilibrium* (i.e., relatively stable flow conditions) and short *disequilibrium* phases (i.e., high-energy flood events with the power to change the course of a stream completely) (Bridge & Demicco, 2008; Limaye & Lamb, 2014; Wohl, 2021). This discharge regime promotes the formation of connected and highly conductive ASG structures that form when streambed sediments accumulate and build up over time during dynamic equilibrium phases, and are subsequently buried during disequilibrium phases (Bridge & Demicco, 2008; Constantz, 2016; Limaye & Lamb, 2014; Siegenthaler & Huggenberger, 1993). As sediment sources remain mostly the same during different flow phases, these buried paleo-channels consist of the same material as the surrounding sediments but differ in that the sediments are more strongly aligned, connected and hydraulically conductive in the direction of streamflow, causing *preferential flow* (Guin et al., 2010; Huggenberger et al., 1998; Langhoff et al., 2006; Siegenthaler & Huggenberger, 1993). Preferential flow not only affects GW flow and solute transport, but also the spatial distribution of exchange fluxes between streams and ASG aquifers (Boano et al., 2014; Cardenas et al., 2004; Huber & Huggenberger, 2016; Huggenberger et al., 1998; Salehin et al., 2004; Schilling, Irvine, et al., 2017), adding to the already convoluted controls on exchange fluxes arising from geomorphology and hydrodynamics in mountainous regions (Larsen et al., 2014; Rhodes et al., 2017; Stonedahl et al., 2013).

Since ASG aquifers consist of mostly the same mix, non-intrusive geophysical techniques (e.g., transient electromagnetics (TEM), electrical resistivity tomography) are not reliable in detecting, delineating, or quantifying preferential flow (Brunner et al., 2017; Linde et al., 2015). Nor are the flow models commonly applied to simulate GW flow in ASG aquifers, as most models fail to reproduce the dynamic interactions between rivers and ASG aquifers, and don't address the anisotropy of ASG sediments (Brunner et al., 2017; Gianni et al., 2019; Schilling, Cook, & Brunner, 2019; Tang et al., 2017). If isotropic conditions are assumed in anisotropic sediments, model calibration leads to parameters compensating for the structural inadequacies of the underlying model, as systematically demonstrated by Gianni et al. (2019). Correctly identifying and reproducing river-aquifer interactions and preferential flow is crucial for GW protection zone delineation, particularly in the context of riverbank filtration (RBF), where GW is pumped right next to rivers and the risk of contamination is thus elevated (Hoehn, 2002; Maliva, 2020).

The few approaches that so far were successful in identifying and quantifying preferential flow through ASG aquifers build on combinations of high-resolution intrusive measurements of sediment structures, complex geostatistical techniques, physically-based flow simulations and computationally demanding inversion approaches (Brunetti et al., 2019; Brunner et al., 2017; Gianni et al., 2019; Jha et al., 2016; Jussel et al., 1994a, 1994b; Linde et al., 2015; Pirot et al., 2015). While such complex and advanced approaches might be successful in certain cases, they are not widely applicable because (a) intrusive measurements (e.g., facies analysis in gravel pits) are unavailable in most situations (Comunian et al., 2011), (b) due to the limits of non-intrusive geophysical techniques, connected subsurface structures are not reliably identified in ASG sediments (Hauser et al., 2017; Meyer et al., 2018), and (c) the complexity of the employed modeling approaches is too demanding for most practical applications (Ramgraber et al., 2020; Zovi et al., 2017).

As shown by Chow et al. (2019), however, it's possible to reproduce the complex surface water-groundwater (SW-GW) dynamics of ASG sites without an overly complex modeling framework or precise prior knowledge of the location of connected subsurface structures. Comparing approaches of varying complexity, they showed that calibrating an integrated surface-subsurface hydrological flow model (ISSHM) (Paniconi & Putti, 2015; Sebben et al., 2013) of a real-world ASG site via regularized pilot point (PP) inversion (Doherty, 2003) against hydraulic head (H) and SW-GW exchange flux observations marks the best trade-off between modeling approaches that are too simple (i.e., too much intrinsic error) or too complex (i.e., too much epistemic error). Complex geostatistical models employing multiple point statistics (MPS) were only more accurate if the image used to train the MPS algorithm was a robust representation of the true subsurface structure and if the flow model calibration data set consisted of large amount of H and SW-GW exchange flux observations, which is rarely the case. Zovi et al. (2017) came to similar conclusions and showed that the uncertainty in buried ASG paleo-channel delineation derived from geophysical data and MPS simulations is too large to produce more accurate simulations compared to much simpler, multi-Gaussian simulations that don't fully respect the connectivity of ASG sediments. Also Tang et al. (2017) concluded that, for simulations of ASG river corridors, multi-Gaussian and non-multi-Gaussian

hydraulic conductivity (K)-fields produce similar results for hydraulically connected stream-aquifer systems. This confirms the findings of Siirila-Woodburn and Maxwell (2015), who investigated how different geostatistical models affect the simulation of GW flow and solute transport through connected heterogeneous media. They found that solute transport was well captured if the underlying geostatistical model was able to create preferential flow structures, no matter whether the underlying model was multi-Gaussian or non-multi-Gaussian.

Aiming to balance methodological complexity and practical simplicity for the identification and quantification of preferential flow in ASG aquifers, we here present a new modeling framework based on three pillars:

1. Integrated surface-subsurface hydrological flow modeling with flow tracking
2. Calibration tailored to reproduce spatially connected, heterogeneous K-fields via spatially varying, preferred anisotropy PP inversion
3. A diverse observation data set containing hydraulic and tracer-based observations

Specifically, we use tracer-based observations of SW-GW exchange fluxes and the fraction of locally infiltrated stream water in the aquifer (f_{stream}) to identify preferential flow paths and combine these observations with H and stream discharge (Q_{SW}) observations into an automated, multivariate calibration of an ISSHM. Calibration is based on PP inversion of aquifer and streambed K-fields, employing a novel approach that introduces spatially varying, preferential directions of anisotropy into the interpolation variograms used for K-field generation. This approach facilitates the calibration of anisotropic K-fields with increased connections in the downvalley and downstream directions and reduces the potential for parameters to compensate for structural inadequacies in the model. We demonstrate the robustness and performance of the framework on a well-studied ASG RBF site in Switzerland and quantify the information content of different observations for the identification of connected subsurface structures.

2. Materials and Methods

2.1. Study Site and Observations

The study site at the outlet of the upper Emme valley, a 194 km² alluvial headwater catchment in the Swiss Pre-Alps (Figure 1a), has already served for multiple hydrogeological studies and is equipped with an extensive monitoring network (Figura et al., 2011, 2013; Käser & Hunkeler, 2015; Kropf et al., 2014; Lapin et al., 2014; Moeck et al., 2022; Peel et al., 2022; Popp et al., 2021; Schilling, Gerber, et al., 2017; Tang et al., 2018). GW is abstracted on a floodplain from 8 wells located 150–250 m away from the Emme river (Figure 1a). The valley is 200–500 m wide and the topographic gradient low (<1%). The aquifer extends 20 km upstream of the RBF well-field and covers 6 km². On average, 0.4 m³/s are abstracted, compared to an average of 4.4 m³/s Q_{SW} and 0.8 m³/s of GW outflow (Käser & Hunkeler, 2015; Würsten, 1991). At the wellfield, the ASG aquifer has an average thickness of 25 m (max: 46 m) and consists of Quaternary alluvial gravel (80%) and sand (20%) (classification: brown gravel (G1) and gray gravel (G2) with some open framework gravel (OF)) (Blau & Muchenberger, 1997; Siegenthaler & Huggenberger, 1993). The aquifer is constrained underneath by impermeable Freshwater Molasses and on the sides by moraines (Blau & Muchenberger, 1997; swisstopo, 2019). Porosity and K of the aquifer (K_{aq}) range from 0.1 to 0.3 (Arbenz et al., 1925; Blau & Muchenberger, 1997; Würsten, 1991) and 200–1,350 m/d (Würsten, 1991), respectively. Porosity and K of the streambed (K_{sb}) range from 0.05 to 0.15 and 1–10 m/d, respectively (Schilling, Gerber, et al., 2017; Tang et al., 2018). Q_{SW} and SW-GW exchange fluxes are highly dynamic, with alternating losing and gaining river sections (Käser & Hunkeler, 2015; Schilling, Gerber, et al., 2017; Tang et al., 2018). The site is a typical example of a low gradient, *dynamic equilibrium-disequilibrium* system ubiquitous in peri-alpine regions. Extended periods of stable flow ($Q_{50} = 2.19$ m³/s) and frequent periods of low flow ($Q_{95} = 0.32$ m³/s) are interrupted by infrequent and short periods of massive overbank flow ($Q_{0.5} = 104$ m³/s) (FOEN, 2020; Smakhtin, 2001). During low flow, sections of the Emme can run dry and abstraction account for 50% of total outflow from the catchment (Käser & Hunkeler, 2015), whereas peak flood events can rearrange and rebuild the streambed morphology and properties completely (Tang et al., 2018).

100 years ago, the RBF wells were constructed inside a buried paleo-channel that was found at a depth of 13–33 m (Arbenz et al., 1925; Gubelmann, 1930). Unfortunately, historic borelogs are not available. The national geological map provides historical stream locations both upstream and downstream of the wellfield, but such information is missing for the wellfield (swisstopo, 2019). The likely reason for this information gap are terrace-forming

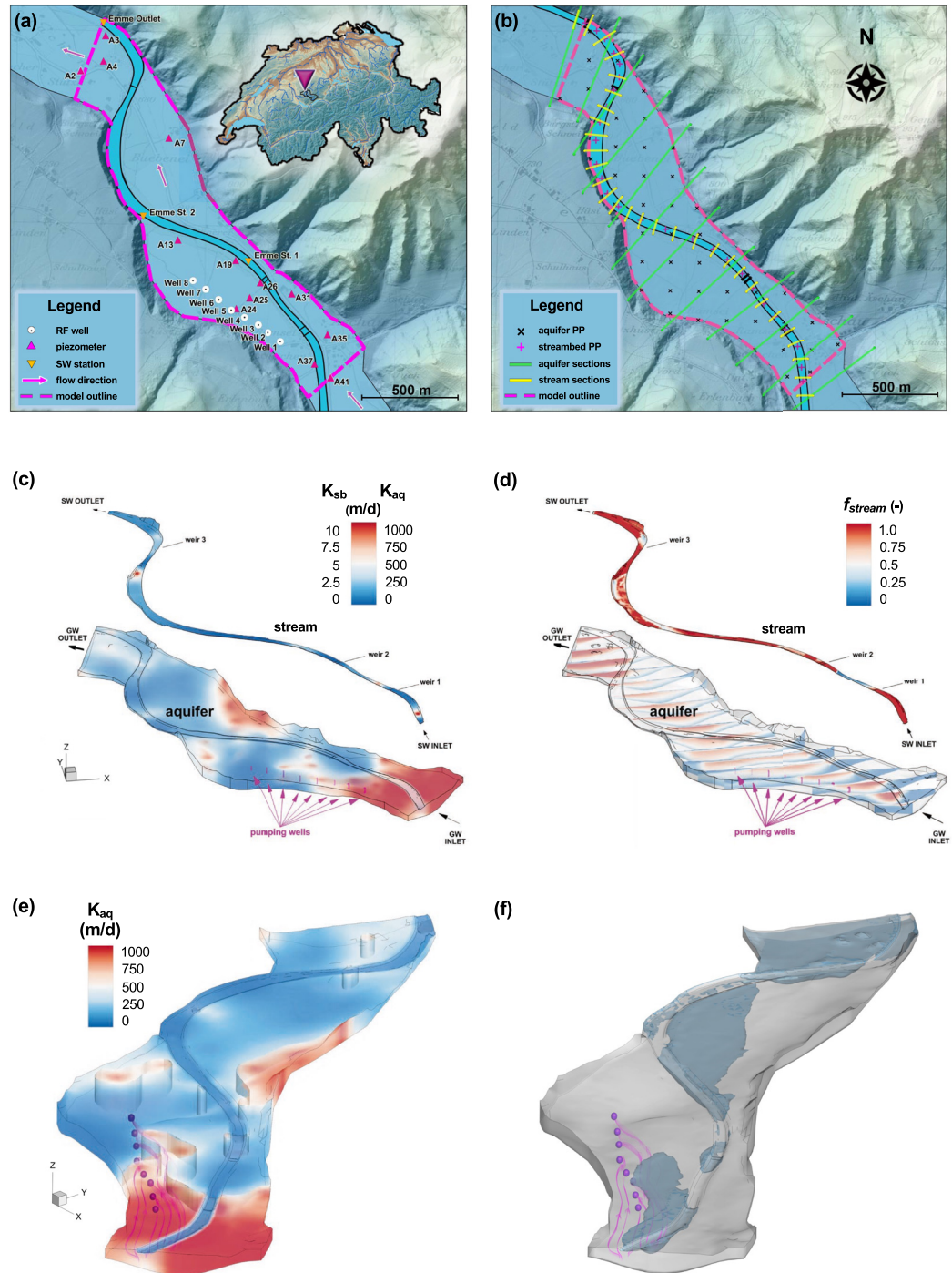


Figure 1. (a) Map of the experimental RBF wellfield and its location inside Switzerland at the Upper Emmental catchment outlet. The Emme River is indicated by thick black outlines (blue infill) and the alluvial sand and gravel aquifer by fine black outlines (semi-transparent, light blue infill). Step weirs in the stream are illustrated by thick black lines perpendicular to the stream. (b) Map of the pilot points (PP) and sections of constant, preferred spatial correlation directions. (c) Calibrated K_{sb} - and K_{aq} -fields. (d) Slice-view of f_{stream} . (e) Preferential flow paths via the buried and connected high- K_{aq} paleochannel structure, illustrated by backwards tracking flowlines from the 8 pumping wells, plotted against a continuously colored K_{aq} -field and a $K_{aq} = 550$ m/d iso-surface highlight. (f) Outline of a plume of 85% or more locally infiltrated stream water (*i.e.*, $f_{stream} = 85\%$ iso-surface). f_{stream} in both (d) and (f) correspond to the state at the end of the transient simulation period (*i.e.*, 06-Feb-2015 23:59).

sediments that overlay the floodplain and stem from a historically active, now insignificant high-gradient creek on the wellfield edge. The site is now interspersed by wellfield infrastructure, powerlines, and sewers, preventing reliable geo-electrical assessment of ASG sediments. Recent tow TEM analyses (Christiansen et al., 2009) hinted at a buried high-K structure, but for >75% of the wellfield the signals were perturbed (Figure S1 in Supporting Information S1). Available borelogs confirm the existence of a buried paleo-channel (classification: G2 and OF) at the reported depth (AWA, 2021), but they are too sparse for reliable paleo-channel delineation. Recent tracer analyses revealed that upstream and downstream wells receive significantly larger f_{stream} compared to mid-section wells, hinting at a meandering, high-K paleo-channel (Popp et al., 2021; Schilling, Gerber, et al., 2017).

The hydraulic dynamics between stream, GW and wells were analyzed in detail during a controlled pumping experiment (Schilling, Gerber, et al. (2017): Following a period of constant maximum pumping at 0.4 m³/s, pumping was halved to 0.23 m³/s for 7 days (26-Jan-2015–02-Feb-2015) before setting it back to 0.4 m³/s, inducing a transient adaption of the hydraulic state to a systematic change of pumping rates. The following observations were recorded:

- H: Hydraulic heads in 13 piezometers
- Q_{out} : SW discharge at the outlet of the catchment
- Q_{EX} : SW discharge upstream and downstream of a gaining section based on dye dilution
- T_R : GW residence times based on ²²²Rn, ³⁷Ar, and ³H/³He radioisotope analyses
- f_{stream} : Fractions of locally infiltrated stream water based on (atmospheric) noble gases

Details and a full list of observations are available from Schilling, Gerber, et al. (2017) and in Text S1 and Table S1 of in Supporting Information S1.

2.2. Flow Model

2.2.1. Conceptual Model and Previous Studies

Herein, we adapted an existing SW-GW flow model of the wellfield by Schilling, Gerber, et al. (2017). The available numerical model was built in the ISSHM HydroGeoSphere (HGS) (Aquanty, 2020). The original model conceptualized the system as a homogeneous aquifer and a distinct, homogeneous streambed covering the top 0.5 m of stream sediments. Exchange fluxes were explicitly simulated and f_{stream} , regional GW and precipitation tracked throughout the wellfield. Model calibration was sequential against GW level, residence time and f_{stream} observations, revealing $K_{aq} = 550$ m/d, $K_{sb} = 2.4$ m/d and porosity = 0.1 as optimal homogeneous parameters. The homogeneous model robustly predicted f_{stream} of an independent pumping and tracer experiment conducted 4 years later (Popp et al., 2021). While Tang et al. (2018) already enhanced the original model by multi-Gaussian, heterogeneous K-fields with Ensemble Kalman filter-based data assimilation (Kurtz et al., 2017), we here also adapt and extend the original model by heterogeneous K-fields, but in contrast to Tang et al. (2018), via a novel, spatially varying, preferred anisotropy PP inversion approach that facilitates the emergence of directional and connected high-K structures.

2.2.2. Numerical Simulator and Model Setup

Numerical simulator: The ISSHM HGS simulates variably-saturated GW flow with Richards' equation utilizing the van Genuchten parameterization, and SW flow with the 2-D diffusion wave approximation to the Saint-Venant equations (Brunner & Simmons, 2011; Therrien & Sudicky, 1996). SW and GW is fully-coupled via the dual-node approach (de Rooij, 2017; Ebel et al., 2009). Water from different origins is tracked throughout the model using a mixing-cell implementation (Partington et al., 2011), enabling direct comparison between observed and simulated f_{stream} . HGS was chosen as it's suited for the simulation of complex SW-GW exchange dynamics (Banks et al., 2011; Irvine et al., 2012; Munz et al., 2017; Schilling et al., 2020; Schomburg et al., 2018), flow over streambed microtopography (Ameli & Creed, 2017; Frei et al., 2010), and winter hydrological processes as prevalent in mountainous river corridors (Ala-Aho et al., 2017; Cochand et al., 2019; Schilling, Park, et al., 2019).

Numerical setup: Floodplain topography is based on the Swiss digital elevation model (DEM) (horizontal resolution: 2 m; vertical resolution: 0.5 m; swisstopo (2021)), streambed topography on an airborne through-water photogrammetry-based DEM (horizontal resolution: 0.25 m; vertical resolution: 0.05 m; Tang et al. (2018)). The top of the aquitard, defined by the DEM of the Freshwater Molasse (AWA, 2021), represents the lower boundary

of the model. The horizontal mesh consists of approximately equilateral triangular elements (side length on floodplain: 17.5 m; within the channel: 8.5 m; elements per layer: 10,983). Vertically, the model is divided into 15 proportional sublayers, with the top 5 layers each covering 0.61%, the next 4 layers 6.1%, and the bottom 6 layers 12% of the vertical model extent. For the average thickness of 25 m, this translates to 0.15 m, 1.5 and 15 m layers, respectively, satisfying the criteria for accurate simulation of variably saturated flow (e.g., Downer and Ogden (2004)). The soil water retention functions and the surface flow properties of the ASG river corridor sediments were parameterized after Dann et al. (2009) and Li et al. (2008). As the small amount of precipitation that fell during the pumping experiment was first stored on the floodplain as snow and then melted gradually, causing only a small amount of local infiltration, overland flow on the floodplain was restricted for faster computation via implementation of a large surface roughness (Schilling, Gerber, et al., 2017). All hydraulic parameters are provided as Table S2 in Supporting Information S1.

Boundary conditions (BC): The model is forced by hourly observations of (a) streamflow measured at a gauging station a few kilometers upstream of the site (second-type BC), (b) regional GW inflow measured at the model's upstream boundary (first-type BC), (c) local precipitation (minus potential evapotranspiration; second-type BC), and (d) pumping (second-type BC). Initial conditions represent the state immediately before the pumping experiment. For more details see Schilling, Gerber, et al. (2017).

2.3. Inverse Model

Calibration: Heterogeneous K-fields were calibrated via PP inversion. In basic PP inversion, values are calibrated only at PP, values of model cells in-between the PP are interpolated from the calibrated PP, for example, with ordinary kriging (Cui et al., 2021; Doherty, 2003; Moeck et al., 2015). Basic PP inversion produces heterogeneous structures without having to calibrate all model cells individually, thereby radically reducing the number of parameters subject to calibration. By employing regularization and subspace methods, inversion can be further stabilized numerically, prior information on the subsurface included in the calibration procedure, and the number of parameters requiring calibration reduced (Alcolea et al., 2006, 2008; Doherty, 2003; Doherty et al., 2010; Moore et al., 2010). By treating aquifer and streambed as two separate hydrofacies with individual PP and interpolation variograms, their structures can be inversely identified independently of one another but based on the same observation data set.

While versatile, basic PP inversion assumes multi-Gaussian distributions for (log-transformed) K-fields, which is not valid for ASG aquifers with non-multi-Gaussian, connected structures such as buried paleo-channels (Gómez-Hernández & Wen, 1995; Kerrou et al., 2008; Khambhammettu et al., 2020). As outlined in the introduction, an often chosen path to tackle this limitation lies in adding more complex geostatistical simulations to the inversion framework (Pirot et al., 2015; Zovi et al., 2017), but this approach is computationally very demanding and only warranted where sufficient detail on the heterogeneity of the subsurface is available – which is rarely the case. Here we present an alternative and more efficient path based on a novel PP inversion approach (Doherty, 2020b; Gallagher & Doherty, 2020): At the heart of the proposed approach lies the use of anisotropic ordinary kriging with the introduction of spatially varying, preferred directions of anisotropy to the interpolation variogram. By using anisotropic ordinary kriging with spatially varying, preferred directions of anisotropy, the emergence of connected structures that follow preferential directions is encouraged, while the underlying approach remains multi-Gaussian. Moreover, rather than defining just one preferred direction of anisotropy for the entire model or larger model zones, spatially varying, preferred directions of anisotropy are automatically calculated for each model element individually based on a quantification of the downstream bearings of each individual model element, with the downstream bearings, for example as in this study, defined by the outlines and downvalley direction of an alluvial valley and the outlines and downstream direction of an alluvial river. Ultimately, for every model element an individual variogram for the interpolation of K from the PP is used.

To limit the potential for unphysical parameter combinations during calibration, which can quickly degrade the numerical stability of ISSHMs, it's strongly recommended to employ regularization (Alcolea et al., 2006, 2008; Doherty, 2003; Doherty & Hunt, 2010; Herrera et al., 2021). Here, stable and highly efficient hybrid subspace regularization (Tikhonov regularization combined with truncated singular value decomposition (SVD; Doherty et al., 2010; Tikhonov & Arsenin, 1977; Tonkin & Doherty, 2005)) was employed. The procedure not only enables stable inversion but further reduces the number of parameters that need to be calibrated, focusing calibration on only the most important principal components (PC) of parameters rather than the base parameters themselves

(Aster et al., 2013; Doherty, 2015). Model inversion was carried out with PEST_HP (Doherty, 2020a). Extended methodological details are described in Text S1 of Supporting Information S1.

Parameters: Aquifer and streambed are considered as separate hydrofacies with individual PP and K-fields. To enable enough spatial detail in the reproduction of the buried paleo-channel and to capture all gaining and losing stream sections, for K_{aq} 73 PP were separated by approximately 125 m and distributed evenly across the model domain, and for K_{sb} 29 PP were spaced at approximately 75 m intervals along the stream centerline (Figure 1b). For the calibration of the K_{aq} -field, horizontal anisotropy in the downvalley direction was defined as the preferred direction (using the Emme valley outlines to define the spatially varying bearings), and for the K_{sb} -field in the direction of streamflow (using the Emme streambanks to define the spatially varying bearings). To enable not only spatially varying directions but also spatially varying scales of anisotropy, the aquifer was divided into 12 sections and the streambed into 30 sections (Figure 1b), with separate anisotropy factors calibrated for each section. As the predominant flow direction in the aquifer is horizontal (Popp et al., 2021; Schilling, Gerber, et al., 2017; Tang et al., 2018), only one vertical anisotropy factor was calibrated for the entire model. By calibrating anisotropy factors, interpolation variograms could vary throughout calibration, thereby ensuring that the maximum amount of information available from the observations is captured during inversion (Doherty, 2015).

Observation weighting scheme: While different observation types (OT) represent processes of different spatial and temporal scales, here they are in their sum equally important for the predictive purpose of the model. To accommodate this, an OT-balanced weighting scheme was employed (Doherty & Welter, 2010; McCallum et al., 2012; Schilling, Cook, & Brunner, 2019). Base weights were defined as the inverse of OT-specific measurement uncertainties and final weights obtained by adjusting these base weights such that each OT contributed on a similar order to the objective function. Since GW level observations were the most numerous, they were used as a reference, and weights of other observations adjusted accordingly. The number of observations, the base and the final weights are provided in Table S2 of in Supporting Information S1 (full observation data set provided in Data set DS1 of in Supporting Information S1).

2.4. Predictive Uncertainty and Data Worth Analyses

Flow of information: How individual observations and OT inform the different parameters subject to calibration was investigated via SVD-based PC analysis of the Jacobi matrix of sensitivities between parameters and model outputs (Doherty, 2015; Hill & Tiedeman, 2007; Schilling et al., 2014).

Predictive uncertainty reduction: Predictive uncertainty reduction achieved through calibration was quantified for selected predictions via Schur's complement-based first order, second moment analysis (Christensen & Doherty, 2008; Dausman et al., 2010; Doherty, 2015; Fienen et al., 2010). By adding different OT to the data set one at a time, all possible OT pairings were evaluated.

Parameter uncertainty reduction: The reduction of parameter uncertainty achieved through calibration was also quantified via Schur's complement and used as a measure of parameter identifiability (Doherty, 2015; Fienen et al., 2010; Guillaume et al., 2019; White et al., 2016). For all data worth uncertainty analyses, the toolbox pyEMU was used (White et al., 2016).

3. Results

3.1. Calibrated Flow Model

Calibration produced a parameter set that reproduced all OT in a balanced manner and according to the weights set for calibration. Detailed root-mean-square-errors (RMSE) between the different observations and corresponding model outputs are provided in Table S2 of Supporting Information S1. While residuals for GW levels and f_{stream} are equally distributed (Figure S2 and S3 in Supporting Information S1), the model is biased towards low discharge (Figure S4 and S5 in Supporting Information S1). However, the bias is small (less than 0.5 m³/s on average) and attributable to being forced to use discharge measurements from a gauging station a few kilometers upstream of the model (see extended discussion in Schilling, Gerber, et al. (2017)).

Calibrated K_{aq} - and K_{sb} -fields and selected model outputs are illustrated in Figures 1c–1f. Overall, the upstream section of the site is more conductive compared to the downstream section. As suspected, a distinct, connected

high-K paleo-channel could be identified for the upstream section of the floodplain (Figures 1c and 1d). Wells 1–4 sit within the paleo-channel, which subsequently meanders around wells 5–7, ends upstream of well 8 and appears again on the downstream end of the floodplain. The paleo-channel causes strong preferential flow in the wellfield, highlighted by backwards-tracking flowlines from the wells against (a) the calibrated K_{aq} -field with a $K_{aq} = 550$ m/d iso-surface (Fig. 1e), and (b) a plume of locally infiltrated stream water represented by an $f_{stream} = 85\%$ iso-surface (Figure 1f). In agreement with the observations and the independent measurements of Popp et al. (2021), the upstream wells 1–3 and downstream wells 6–8 receive water primarily via the paleo-channel, whereas the mid-section wells 4 and 5 receive more regional GW (illustrated by flowlines in Figures 1e and 1f). Rather than K, the dominant control on exchange fluxes are the weirs, with the most complex patterns arising where the aquifer is thinnest (Figures 1c, 1d, and 1f).

3.2. Predictive Uncertainty and Data Worth Analyses

Flow of information: Altogether, the 14 parameter PC that were calibrated explain more than 99.5% of the total variance encapsulated in the observation data set, with the most important two explaining more than 84% (PC1: 71.7%; PC2: 12.6%). The loadings of PC1 and PC2 are dominated by K_{aq} , K_{sb} and horizontal anisotropy factors at PP in the upstream two thirds of the wellfield, as well as the single vertical anisotropy value (Figure 2b). The two corresponding, most important observation PC are dominated in their loadings by observations of f_{stream} (triangles in Figure 2a) and, to a lesser degree, Q_{out} (diamonds in Figure 2a). This reveals the large importance of f_{stream} observations for informing K_{aq} and K_{sb} . Despite their large number and considerable spatial and temporal coverage, the information content of classic H observations for the calibration of the heterogeneous K_{aq} - and K_{sb} -fields is thus small, while the information content of even just a few tracer-based OT is very large.

Parameter uncertainty reduction: The largest reduction of parameter uncertainty was achieved in the upstream section of the model domain (Figures 2c and 2d). Mirroring the flow of information analysis (Figures 2a and 2b), the largest reduction in uncertainty for K_{aq} was achieved at PP upstream of the f_{stream} measurement locations, and for K_{sb} upstream of the Q_{EX} measurement locations (Figure 1; Figures 2c and 2d). The location of the buried paleo-channel coincides with the zone where most data are available and where the largest reductions in parameter uncertainty were achieved. This highlights the information content of a combined hydraulic and tracer-based data set for the detection of preferential flow-causing connected subsurface structures.

Predictive uncertainty reduction: The predictive uncertainty reduction was evaluated for predictions of (a) f_{stream} in selected abstraction wells and (b) Q_{EX} at the two Emme measurement locations. Predictions were made 1 week into the future, measured from the end of the transient pumping experiment. A summary for every possible combination of OT is provided in Figure 2e. Comparing the post- to the pre-calibration predictive uncertainty standard deviation demonstrates that, for any combination of OT and at any location, calibration reduces the predictive uncertainty significantly. However, clear differences in the predictive uncertainty reduction potential of different OT exist. The uncertainty of predictions of Q_{EX} would be reduced more by calibration against a flux-based OT (i.e., Q_{out} , Q_{EX} and f_{stream}) compared to calibration against H observations. However, if two or more OT were combined, predictive uncertainty reductions for Q_{EX} predictions converge. For predictions of f_{stream} , calibration against direct observations of f_{stream} achieves an uncertainty reduction by a factor of 200, while calibration against observations of H, Q_{EX} and Q_{out} , or combinations thereof, achieves a reduction by factors of 2–10 only. Interestingly, predictive uncertainty reduction for f_{stream} is larger in wells 5 and 7 compared to well 1, indicating how an increasing number of tracer-based observations upstream of a location used for predictions provides cumulative information.

4. Discussion

Multi-Gaussian, anisotropy-constrained inversion of an ISSHM against a multivariate set of hydraulic and tracer-based observations allowed a connected paleo-channel, hinted at in historic reports, geological maps, and geophysical data, to be reproduced. This highly permeable paleo-channel was reproduced even though regularization employed a homogeneous aquifer and streambed and no direct information on the shape or location of the paleo-channel was provided to the inversion. The clearest outlines of a paleo-channel emerged in the upstream section of the wellfield, for which cumulatively the largest amount of tracer-based information was available. In contrast, for areas where only hydraulic head and stream discharge observations were available, connected

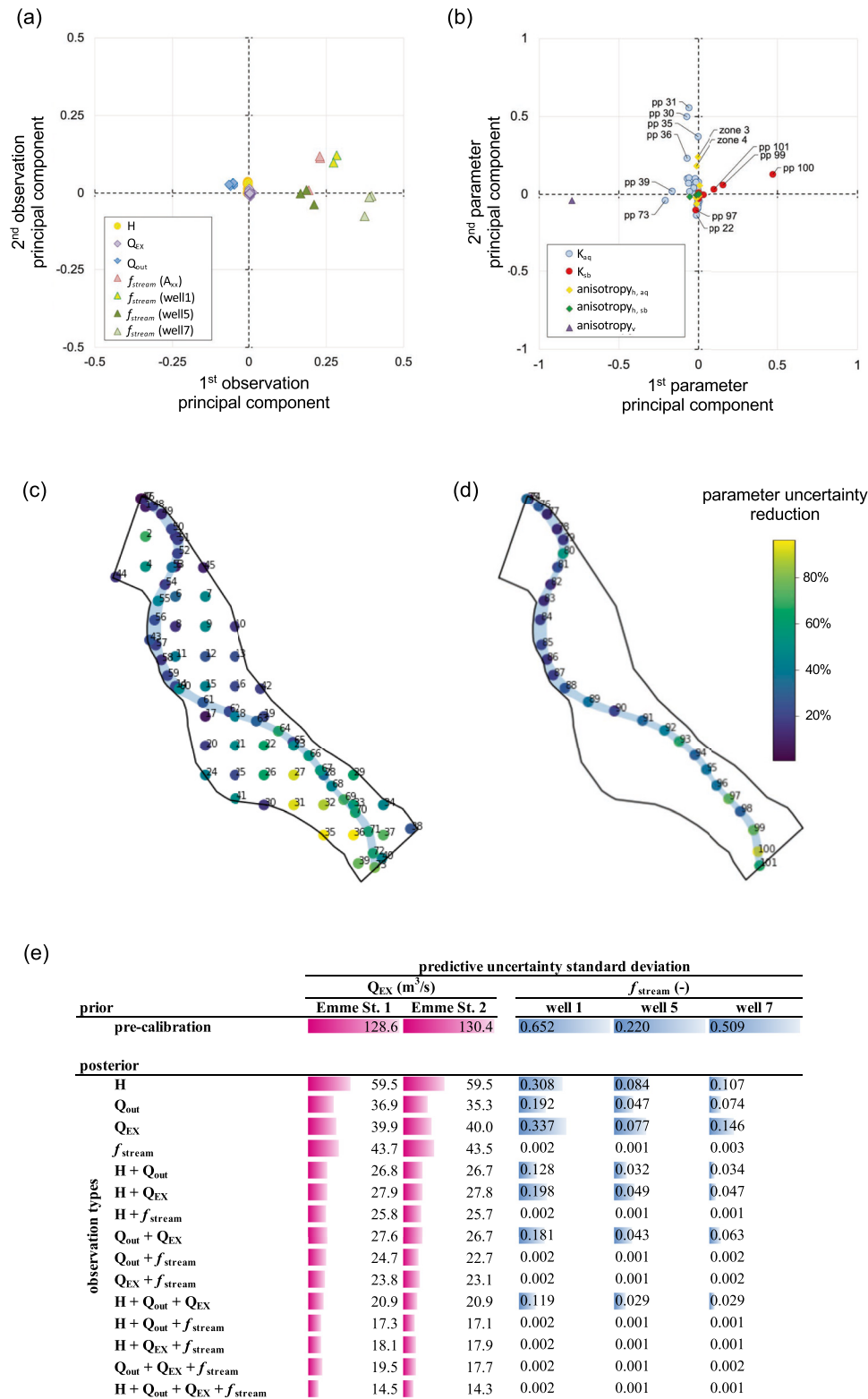


Figure 2. Flow of information and parameter identifiability. (a) first and second principal components (PC) of the observations data set. (b) first and second PC of the calibrated model parameters. (c) Reduction of parameter uncertainty in percent for K_{sq} at PP. (d) Reduction of parameter uncertainty in percent for K_{sb} at PP. PP numbers (pp #) in (a) and (b) correspond to the numbers indicated in (c) and (d). (e) Predictive uncertainty standard deviation of different predictions pre- (prior) and post-calibration (posterior) for the actual (i.e., $H + Q_{out} + Q_{EX} + f_{stream}$) and all hypothetically possible observation type combinations. Color bars represent normalized predictive uncertainty, with the pre-calibration uncertainty being defined as 100%.

subsurface structures couldn't be robustly identified. This limitation, however, also applies to more complex modeling approaches (Chow et al., 2019; Zovi et al., 2017). For reliable identification of connected subsurface structures, observations able to capture preferential flow, that is, exchange fluxes and the fraction of locally infiltrated stream water, are necessary, confirming previous findings (Delottier et al., 2016; Hunt et al., 2006; Partington et al., 2020; Sanford, 2011; Schilling, Cook, & Brunner, 2019; Thiros et al., 2021).

Although based on an ISSHM and sophisticated multivariate model calibration, the new modeling framework is simpler than previous approaches to model flow through complex, anisotropic ASG aquifers, as it doesn't require advanced geostatistical modeling or precise knowledge on the location of connected subsurface structures. The crucial geological constraints that need to be imposed onto the inversion procedure – spatially-varying, preferred anisotropy directions – are readily observable from the outlines of streams and river corridors. As opposed to the calibration employed for the vast majority of models simulating alluvial SW-GW systems (Gianni et al., 2019), our approach provides a receptacle for the systematic anisotropies in ASG sediments, thereby avoiding a systematic shortcoming and bias in existing approaches. While the modeling framework can reproduce principal preferential flow paths and associated paleo-channels, reproducing multi-layered and intersecting subsurface channel networks encountered in wide braided river systems likely necessitates more complex geostatistical approaches (Brunetti et al., 2019; Pirot et al., 2015; Renard & Allard, 2013; Siirila-Woodburn & Maxwell, 2015). A promising way forward for the detection of paleo-channels are machine learning-based approaches, which may allow including additional information into the modeling framework while simultaneously reducing the computational burden of ISSHM inversion (Sun, 2018; Wang et al., 2021; Zhan et al., 2022; Zhu & Zabarar, 2018).

5. Conclusions

A critical challenge for groundwater wellhead protection in ASG aquifers are the identification and quantification of the impact of highly permeable, connected subsurface structures such as buried paleo-channels that facilitate and accelerate water and solute transport. Aiming to reduce methodological complexity and to provide a robust and practical modeling approach for identifying and quantifying preferential transport in ASG aquifers, we demonstrated a new framework that builds on (a) integrated surface-subsurface hydrological modeling, (b) inversion which explicitly takes spatially varying, preferred directions of anisotropy into account, and (c) a calibration data set consisting of hydraulic and tracer-based observations. The successful delineation of a real-world buried paleo-channel and unraveled information content of the different OT highlights the importance of taking the anisotropy of sediments into account in river corridor simulations. This challenges the notion that only complex geostatistical approaches can reproduce preferential flow and has implications for alluvial wellfield management, as it demonstrates that tracer-based observations in combination with anisotropy-constrained inversion of a flow model are necessary to efficiently protect our drinking water resources. With the recent advances in analytical on-site and computational techniques (Brunner et al., 2017; Hartmann et al., 2021; Sahraei et al., 2020; Schilling et al., 2021), however, tracer-aided ISSHM modeling is now widely applicable, affordable and reliable.

Data Availability Statement

All observation data used in this study were published in Schilling, Gerber, et al. (2017). All model input files required to run the calibrated model for the duration of the pumping experiment are supplied alongside the full list of observations and associated weights as Data set DS1 in Supporting Information S1, available for download from HydroShare, under <https://doi.org/10.4211/hs.61bb11e383034bc194f85a57a1d251eb> (Schilling et al., 2022).

References

- Ala-Aho, P., Soulsby, C., Wang, H., & Tetzlaff, D. (2017). Integrated surface-subsurface model to investigate the role of groundwater in headwater catchment runoff generation: A minimalist approach to parameterisation. *Journal of Hydrology*, 547, 664–677. <https://doi.org/10.1016/j.jhydrol.2017.02.023>
- Alcolea, A., Carrera, J., & Medina, A. (2006). Pilot points method incorporating prior information for solving the groundwater flow inverse problem. *Advances in Water Resources*, 29(11), 1678–1689. <https://doi.org/10.1016/j.advwatres.2005.12.009>
- Alcolea, A., Carrera, J., & Medina, A. (2008). Regularized pilot points method for reproducing the effect of small scale variability: Application to simulations of contaminant transport. *Journal of Hydrology*, 355(1–4), 76–90. <https://doi.org/10.1016/j.jhydrol.2008.03.004>
- Ameli, A. A., & Creed, I. F. (2017). Quantifying hydrologic connectivity of wetlands to surface water systems. *Hydrology and Earth System Sciences*, 21, 1791–1808. <https://doi.org/10.5194/hess-21-1791-2017>

Acknowledgments

The authors would like to thank the Wasserverbund Regio Bern AG for their support, and kindly acknowledge the funding received via the Swiss National Science Foundation (SNSF) project grant 200021_179017. Open access funding provided by Universite de Neuchâtel.

- Aquanty, I. (2020). *HydroGeoSphere. A three-dimensional numerical model describing fully integrated subsurface and surface flow and solute transport*. Waterloo, Aquanty, Inc.
- Arbenz, P., Freiburghaus, J., & Peter, H. (1925). *Expertenbericht zu Handen der Baudirektion des Kantons Bern betreffend Wasserableitung aus dem Emmental durch die Stadt Bern*. Bern.
- Aster, R. C., Borchers, B., & Thurber, C. H. (2013). *Parameter estimation and inverse problems* (Vol. 90). Academic Press.
- AWA. (2021). *GEOLOG: Basic geological data*. Amt für Wasser und Abfall des Kantons Bern (AWA).
- Banks, E. W., Brunner, P., & Simmons, C. T. (2011). Vegetation controls on variably saturated processes between surface water and groundwater and their impact on the state of connection. *Water Resources Research*, 47. <https://doi.org/10.1029/2011WR010544>
- Bayer, P., Huggenberger, P., Renard, P., & Comunian, A. (2011). Three-dimensional high resolution fluvio-glacial aquifer analog: Part 1: Field study. *Journal of Hydrology*, 405, 1–9. <https://doi.org/10.1016/j.jhydrol.2011.03.038>
- Blau, R. V., & Muchenberger, F. (1997). *Grundlagen für Schutz und Bewirtschaftung der Grundwasser des Kantons Bern: Nutzungs-, Schutz- und Überwachungskonzept für die Grundwasserleiter des obersten Emmentals, zwischen Emmenmatt, Langnau und Eggwil, Synthesebericht*. Wasser- und Energiewirtschaft des Kantons Bern.
- Boano, F., Harvey, J. W., Marion, A., Packman, A. I., Revelli, R., Ridolfi, L., & Wörman, A. (2014). Hyporheic flow and transport processes: Mechanisms, models, and biogeochemical implications. *Reviews of Geophysics*, 52, 603–679. <https://doi.org/10.1002/2012RG000417>
- Bridge, J. S., & Demicco, R. V. (2008). Rivers, alluvial plains, and fans. In J. S. Bridge & R. V. Demicco (Eds.), *Earth surface processes, land-forms and sediment deposits*. Cambridge University Press.
- Brunetti, C., Bianchi, M., Pirot, G., & Linde, N. (2019). Hydrogeological model selection among complex spatial priors. *Water Resources Research*, 55, 6729–6753. <https://doi.org/10.1029/2019WR024840>
- Brunner, P., & Simmons, C. T. (2011). HydroGeoSphere: A fully integrated, physically based hydrological model. *Ground Water*, 50(2), 170–176. <https://doi.org/10.1111/j.1745-6584.2011.00882.x>
- Brunner, P., Therrien, R., Renard, P., Simmons, C. T., & Hendricks Franssen, H.-J. (2017). Advances in understanding river - Groundwater interactions. *Reviews of Geophysics*, 55(3), 818–854. <https://doi.org/10.1002/2017RG000556>
- Cardenas, M. B., Wilson, J. L., & Zlotnik, V. A. (2004). Impact of heterogeneity, bed forms, and stream curvature on subchannel hyporheic exchange. *Water Resources Research*, 40(8). <https://doi.org/10.1029/2004WR003008>
- Chow, R., Bennett, J., Dugge, J., Wöhling, T., & Nowak, W. (2019). Evaluating subsurface parameterization to simulate hyporheic exchange: The Steinalach River Test Site. *Ground Water*, 58(1), 93–109. <https://doi.org/10.1111/gwat.12884>
- Christensen, S., & Doherty, J. (2008). Predictive error dependencies when using pilot points and singular value decomposition in groundwater model calibration. *Advances in Water Resources*, 31(4), 674–700. <https://doi.org/10.1016/j.advwatres.2008.01.003>
- Christiansen, A. V., Auken, E., & Sørensen, K. I. (2009). The transient electromagnetic method. In R. Kirsch (Ed.), *Groundwater geophysics*. Springer.
- Cochand, F., Therrien, R., & Lemieux, J.-M. (2019). Integrated hydrological modeling of climate change impacts in a snow-influenced catchment. *Ground Water*, 57(1), 3–20. <https://doi.org/10.1111/gwat.12848>
- Comunian, A., Renard, P., Straubhaar, J., & Bayer, P. (2011). Three-dimensional high resolution fluvio-glacial aquifer analog - Part 2: Geostatistical modeling. *Journal of Hydrology*, 405, 10–23. <https://doi.org/10.1016/j.jhydrol.2011.03.037>
- Constantz, J. (2016). Streambeds merit recognition as a scientific discipline. *WIREs Water*, 3, 13–18. <https://doi.org/10.1002/wat2.1119>
- Cui, T., Srekanth, J., Pickett, T., Rassam, D., Gilfedder, M., & Barrett, D. (2021). Impact of model parameterization on predictive uncertainty of regional groundwater models in the context of environmental impact assessment. *Environmental Impact Assessment Review*, 90, 106620. <https://doi.org/10.1016/j.eiar.2021.106620>
- Dann, R., Close, M., Flintoft, M., Hector, R., Barlow, H., Thomas, S., & Francis, G. (2009). Characterization and estimation of hydraulic properties in an alluvial gravel vadose zone. *Vadose Zone Journal*, 8(3), 651–663. <https://doi.org/10.2136/vzj2008.0174>
- Dausman, A. M., Doherty, J., Langevin, C. D., & Sukop, M. C. (2010). Quantifying data worth toward reducing predictive uncertainty. *Ground Water*, 48(5), 729–740. <https://doi.org/10.1111/j.1745-6584.2010.00679.x>
- de Rooij, R. (2017). New insights into the differences between the dual node approach and the common node approach for coupling surface-subsurface flow. *Hydrology and Earth System Sciences*, 21, 5709–5724. <https://doi.org/10.5194/hess-21-5709-2017>
- Delottier, H., Pryet, A., & Dupuy, A. (2016). Why should practitioners be concerned about predictive uncertainty of groundwater management models? *Water Resources Management*, 31(1), 61–73. <https://doi.org/10.1007/s11269-016-1508-2>
- Doherty, J. (2003). Ground water model calibration using pilot points and regularization. *Ground Water*, 41(2), 170–177. <https://doi.org/10.1111/j.1745-6584.2003.tb02580.x>
- Doherty, J. (2015). *Calibration and uncertainty analysis for complex environmental models PEST: Complete theory and what it means for modeling the real world*. Watermark Numerical Computing.
- Doherty, J. (2020a). *PEST_HP. PEST for highly parallelized computing environments*. Watermark Numerical Computing.
- Doherty, J. (2020b). *PLPROC - a parameter list processor*. Watermark Numerical Computing.
- Doherty, J., Fienen, M. N., & Hunt, R. J. (2010). *Approaches to highly parameterized inversion: Pilot-Point theory, guidelines, and research directions*. U.S. Geological Survey.
- Doherty, J., & Hunt, R. J. (2010). *Approaches to highly parameterized inversion: A guide to using PEST for groundwater-model calibration*. U.S. Geological Survey.
- Doherty, J., & Welter, D. (2010). A short exploration of structural noise. *Water Resources Research*, 46. <https://doi.org/10.1029/2009WR008377>
- Downer, C. W., & Ogden, F. L. (2004). Appropriate vertical discretization of Richards' equation for two-dimensional watershed-scale modelling. *Hydrological Processes*, 18, 1–22. <https://doi.org/10.1002/hyp.1306>
- Ebel, B. A., Mirus, B. B., Heppner, C. S., VanderKwaak, J. E., & Loague, K. (2009). First-order exchange coefficient coupling for simulating surface water-groundwater interactions: Parameter sensitivity and consistency with a physics-based approach. *Hydrological Processes*, 23(13), 1949–1959. <https://doi.org/10.1002/hyp.7279>
- Fienen, M. N., Doherty, J., Hunt, R. J., & Reeves, J. (2010). *Using prediction uncertainty analysis to design hydrologic monitoring networks: Example applications from the great lakes water availability pilot project* (Vol. 2010–5159). U.S. Geological Survey.
- Figura, S., Livingstone, D. M., Hoehn, E., & Kipfer, R. (2011). Regime shift in groundwater temperature triggered by the Arctic Oscillation. *Geophysical Research Letters*, 38, L23401. <https://doi.org/10.1029/2011GL049749>
- Figura, S., Livingstone, D. M., & Kipfer, R. (2013). Competing controls on groundwater oxygen concentrations revealed in multidecadal time series from riverbank filtration sites. *Water Resources Research*, 49, 7411–7426. <https://doi.org/10.1002/2013WR013750>
- FOEN. (2020). *Floodstatistics report national gauging station no. 2409 'Emme - Eggwil, Heidbüel' (in German)*. Bern: Swiss Federal Office for the Environment (FOEN).

- Frei, S., Lischied, G., & Fleckenstein, J. H. (2010). Effects of micro-topography on surface–subsurface exchange and runoff generation in a virtual riparian wetland — A modeling study. *Advances in Water Resources*, 33(11), 1388–1401. <https://doi.org/10.1016/j.advwatres.2010.07.006>
- Gallagher, M., & Doherty, J. (2020). *Water supply security for the township of Biggenden: A GMSI worked example report*. National Centre for Groundwater Research and Training, Flinders University.
- Gianni, G., Doherty, J., & Brunner, P. (2019). Conceptualization and calibration of anisotropic alluvial systems: Pitfalls and biases. *Groundwater*, 57(3), 409–419. <https://doi.org/10.1111/gwat.12802>
- Gómez-Hernández, J. J., & Wen, X.-H. (1995). Multigaussian models: The danger of parsimony. *Journal of the Italian Statistical Society*, 4, 167–181. <https://doi.org/10.1007/BF02589100>
- Gubelmann, H. (1930). *Die neue grundwasser-fassungsanlage der wasserversorgung der stadt Bern (in German)*. Bern: Schweizerischer Verein von Gas-und Wasserfachmänner.
- Guillaume, J. H. A., Jakeman, J. D., Marsili-Libelli, S., Asher, M., Brunner, P., Croke, B., et al. (2019). Introductory overview of identifiability analysis: A guide to evaluating whether you have the right type of data for your modeling purpose. *Environmental Modelling & Software*, 119, 418–432. <https://doi.org/10.1016/j.envsoft.2019.07.007>
- Guin, A., Ramanathan, R., Ritzi, R. W., Dominic, D. F., Lunt, I. A., Scheibe, R. D., & Freedman, V. L. (2010). Simulating the heterogeneity in braided channel belt deposits: 2. Examples of results and comparison to natural deposits. *Water Resources Research*, 46(4), W04516. <https://doi.org/10.1029/2009wr008112>
- Hartmann, A., Jasechko, S., Gleeson, T., Wada, Y., Andreo, B., Barberá, J. A., et al. (2021). Risk of groundwater contamination widely underestimated because of fast flow into aquifers. *Proceedings of the National Academy of Sciences of the United States of America*, 118(20), e2024492118. <https://doi.org/10.1073/pnas.2024492118>
- Hauser, J., Wellmann, F., & Trefry, M. (2017). Water table uncertainties due to uncertainties in structure and properties of an unconfined aquifer. *Ground Water*, 56(2), 251–265. <https://doi.org/10.1111/gwat.12577>
- Herrera, P. A., Marazuela, M. A., & Hofmann, T. (2021). Parameter estimation and uncertainty analysis in hydrological modeling. *WIREs Water*, 9(1), e1569. <https://doi.org/10.1002/wat2.1569>
- Hill, M. C., & Tiedeman, C. R. (2007). *Effective groundwater model calibration: With analysis of data, sensitivities, predictions, and uncertainty*. John Wiley & Sons, Inc.
- Hoehn, E. (2002). Hydrogeological issues of riverbank filtration - A review. In C. Ray (Ed.), *Riverbank filtration: Understanding contaminant biogeochemistry and pathogen removal* (Vol. 14). Springer.
- Huber, E., & Huggenberger, P. (2016). Subsurface flow mixing in coarse, braided river deposits. *Hydrology and Earth System Sciences*, 20, 2035–2046. <https://doi.org/10.5194/hess-20-2035-2016>
- Huggenberger, P., Epting, J., & Scheidler, S. (2013). Concepts for the sustainable management of multi-scale flow systems: The groundwater system within the laufen basin, Switzerland. *Environmental Earth Sciences*, 69, 645–661. <https://doi.org/10.1007/s12665-013-2308-0>
- Huggenberger, P., Hoehn, E., Beschta, R., & Woessner, W. (1998). Abiotic aspects of channels and floodplains in riparian ecology. *Freshwater Biology*, 40, 407–425. <https://doi.org/10.1046/j.1365-2427.1998.00371.x>
- Hunt, R. J., Feinstein, D. T., Pint, C. D., & Anderson, M. P. (2006). The importance of diverse data types to calibrate a watershed model of the Trout Lake Basin, Northern Wisconsin, USA. *Journal of Hydrology*, 321, 286–296. <https://doi.org/10.1016/j.jhydrol.2005.08.005>
- Irvine, D. J., Brunner, P., Hendricks Franssen, H.-J., & Simmons, C. T. (2012). Heterogeneous or homogeneous? Implications of simplifying heterogeneous streambeds in models of losing streams. *Journal of Hydrology*, 424–425, 16–23. <https://doi.org/10.1016/j.jhydrol.2011.11.051>
- Jha, S. K., Mariethoz, G., Mathews, G., Vial, J., & Kelly, B. F. J. (2016). Influence of alluvial morphology on upscaled hydraulic conductivity. *Ground Water*, 54(3), 384–393. <https://doi.org/10.1111/gwat.12378>
- Jussel, P., Stauffer, F., & Dracos, T. (1994a). Transport modeling in heterogeneous aquifers: 1. Statistical description and numerical generation of gravel deposits. *Water Resources Research*, 30(6), 1803–1817. <https://doi.org/10.1029/94WR00162>
- Jussel, P., Stauffer, F., & Dracos, T. (1994b). Transport modeling in heterogeneous aquifers: 2. Three-Dimensional transport model and stochastic numerical tracer experiments. *Water Resources Research*, 30(6), 1819–1831. <https://doi.org/10.1029/94WR00163>
- Käser, D., & Hunkeler, D. (2015). Contribution of alluvial groundwater to the outflow of mountainous catchments. *Water Resources Research*, 52(2), 680–697. <https://doi.org/10.1002/2014WR016730>
- Kerrou, J., Renard, P., Hendricks Franssen, H.-J., & Lunati, I. (2008). Issues in characterizing heterogeneity and connectivity in non-multiGaussian media. *Advances in Water Resources*, 31(1), 147–159. <https://doi.org/10.1016/j.advwatres.2007.07.002>
- Khambhammettu, P., Renard, P., & Doherty, J. (2020). The traveling pilot point method. A novel approach to parameterize the inverse problem for categorical fields. *Advances in Water Resources*, 138, 103556. <https://doi.org/10.1016/j.advwatres.2020.103556>
- Kropf, P., Schiller, E., Brunner, P., Schilling, O. S., Hunkeler, D., & Lapin, A. (2014). Wireless mesh networks and cloud computing for real time environmental simulation. *Paper presented at the 10th International Conference on Computing and Information Technology (IC2IT2014)*.
- Kurtz, W., Lapin, A., Schilling, O. S., Tang, Q., Schiller, E., Braun, T., et al. (2017). Integrating hydrological modelling, data assimilation and cloud computing for real-time management of water resources. *Environmental Modelling & Software*, 93, 418–435. <https://doi.org/10.1016/j.envsoft.2017.03.011>
- Langhoff, J. H., Rasmussen, K. R., & Christensen, S. (2006). Quantification and regionalization of groundwater–surface water interaction along an alluvial stream. *Journal of Hydrology*, 320, 342–358. <https://doi.org/10.1016/j.jhydrol.2005.07.040>
- Lapin, A., Schiller, E., Kropf, P., Schilling, O. S., Brunner, P., Jamakovic-Kapic, A., et al. (2014). Real-time environmental monitoring for cloud-based hydrogeological modelling with hydroGeoSphere. *Paper presented at the High performance computing and communications conference*. IEEE HPCC14.
- Larsen, L. G., Harvey, J. W., & Maglio, M. M. (2014). Dynamic hyporheic exchange at intermediate timescales: Testing the relative importance of evapotranspiration and flood pulses. *Water Resources Research*, 50(1), 318–335. <https://doi.org/10.1002/2013WR014195>
- Li, Q., Unger, A. J. A., sudicky, E. A., Kassenaar, D., Wexler, E. J., & Shikaze, S. (2008). Simulating the multi-seasonal response of a large-scale watershed with a 3D physically-based hydrologic model. *Journal of Hydrology*, 357, 317–336. <https://doi.org/10.1016/j.jhydrol.2008.05.024>
- Limaye, A. B. S., & Lamb, P. (2014). Numerical simulations of bedrock valley evolution by meandering rivers with variable bank material. *Journal of Geophysical Research: Earth Surface*, 119, 927–950. <https://doi.org/10.1002/2013JF002997>
- Linde, N., Renard, P., Mukerji, T., & Caers, J. (2015). Geological realism in hydrogeological and geophysical inverse modeling: A review. *Advances in Water Resources*, 86, 86–101. <https://doi.org/10.1016/j.advwatres.2015.09.019>
- Maliva, R. G. (2020). Riverbank filtration. In R. G. Maliva (Ed.), *Anthropogenic aquifer recharge*. Springer.
- McCallum, J. L., Cook, P. G., Berhane, D., Rumpf, C., & McMahon, G. A. (2012). Quantifying groundwater flows to streams using differential flow gaugings and water chemistry. *Journal of Hydrology*, 416–417, 118–132. <https://doi.org/10.1016/j.jhydrol.2011.11.040>

- Meyer, R., Engesgaard, P., Høyer, A.-S., Jørgensen, F., Vignoli, G., & Sonnenborg, T. O. (2018). Regional flow in a complex coastal aquifer system: Combining voxel geological modelling with regularized calibration. *Journal of Hydrology*, 562, 544–563. <https://doi.org/10.1016/j.jhydrol.2018.05.020>
- Moeck, C., Hunkeler, D., & Brunner, P. (2015). Tutorials as a flexible alternative to GUIs: An example for advanced model calibration using Pilot Points. *Environmental Modelling & Software*, 66, 78–86. <https://doi.org/10.1016/j.envsoft.2014.12.018>
- Moeck, C., Schilling, O. S., Künze, R., Brunner, O., & Schirmer, M. (2022). Grundwasser-Modellierung: Warum Unsicherheiten zu quantifizieren sind. *Aqua & Gas*, 7+8. https://www.aquaetgas.ch/de/wasser/trinkwasser-grundwasser/20220628_ag7_warum-modellunsicherheit-en-quantifiziert-werden-sollten/
- Moore, C., Wöhling, T., & Doherty, J. (2010). Efficient regularization and uncertainty analysis using a global optimization methodology. *Water Resources Research*, 46. <https://doi.org/10.1029/2009WR008627>
- Munz, M., Oswald, S. E., & Schmidt, C. (2017). Coupled long-term simulation of reach-scale water and heat fluxes across the river-groundwater interface for retrieving hyporheic residence times and temperature dynamics. *Water Resources Research*, 53, 8900–8924. <https://doi.org/10.1002/2017WR020667>
- Paniconi, C., & Putti, M. (2015). Physically based modeling in catchment hydrology at 50: Survey and outlook. *Water Resources Research*, 51, 7090–7129. <https://doi.org/10.1002/2015WR017780>
- Partington, D., Brunner, P., Simmons, C. T., Therrien, R., Werner, A. D., Dandy, G. C., & Maier, H. R. (2011). A hydraulic mixing-cell method to quantify the groundwater component of streamflow within spatially distributed fully integrated surface water-groundwater flow models. *Environmental Modelling & Software*, 26, 886–898. <https://doi.org/10.1016/j.envsoft.2011.02.007>
- Partington, D., Knowling, M. J., Simmons, C. T., Cook, P. G., Xie, Y., Iwanaga, T., & Bouchez, C. (2020). Worth of hydraulic and water chemistry observation data in terms of the reliability of surface water-groundwater exchange flux predictions under varied flow conditions. *Journal of Hydrology*, 590, 125441. <https://doi.org/10.1016/j.jhydrol.2020.125441>
- Peel, M., Kipfer, R., Hunkeler, D., & Brunner, P. (2022). Variable ^{222}Rn emanation rates in an alluvial aquifer: Limits on using ^{222}Rn as a tracer of surface water – Groundwater interactions. *Chemical Geology*, 599, 120829. <https://doi.org/10.1016/j.chemgeo.2022.120829>
- Pirot, G., Renard, P., Huber, E., Straubhaar, J., & Huggenberger, P. (2015). Influence of conceptual model uncertainty on contaminant transport forecasting in braided river aquifers. *Journal of Hydrology*, 531, 124–141. <https://doi.org/10.1016/j.jhydrol.2015.07.036>
- Popp, A. L., Pardo-Álvarez, Á., Schilling, O. S., Scheidegger, A., Musy, S., Peel, M., et al. (2021). A framework for untangling transient groundwater mixing and travel times. *Water Resources Research*, 57(4), e2020WR028362. <https://doi.org/10.1029/2020WR028362>
- Ramgraber, M., Camporese, M., Renard, P., Salandin, P., & Schirmer, M. (2020). Quasi-online groundwater model optimization under constraints of geological consistency based on iterative importance sampling. *Water Resources Research*, 56(6), e2019WR026777. <https://doi.org/10.1029/2019WR026777>
- Renard, P., & Allard, D. (2013). Connectivity metrics for subsurface flow and transport. *Advances in Water Resources*, 51, 168–196. <https://doi.org/10.1016/j.advwatres.2011.12.001>
- Rhodes, K. A., Proffitt, T., Rowley, T., Knappett, P. S. K., Montiel, D., Dimova, N., et al. (2017). The Importance of bank storage in supplying baseflow to rivers flowing through compartmentalized, alluvial aquifers. *Water Resources Research*, 53, 10539–10557. <https://doi.org/10.1002/2017WR021619>
- Sahraei, A., Kraft, P., Windhorst, D., & Breuer, L. (2020). High-resolution, in situ monitoring of stable isotopes of water revealed insight into hydrological response behavior. *Water*, 12(2), 565. <https://doi.org/10.3390/w12020565>
- Salehin, M., Packman, A. I., & Paradis, M. (2004). Hyporheic exchange with heterogeneous streambeds: Laboratory experiments and modeling. *Water Resources Research*, 40(11), W11504. <https://doi.org/10.1029/2003WR002567>
- Sanford, W. E. (2011). Calibration of models using groundwater age. *Hydrogeology Journal*, 19, 13–16. <https://doi.org/10.1007/s10040-010-0637-6>
- Schilling, O. S., Cook, P. G., & Brunner, P. (2019). Beyond classical observations in hydrogeology: The advantages of including exchange flux, temperature, tracer concentration, residence time and soil moisture observations in groundwater model calibration. *Reviews of Geophysics*, 57(1), 146–192. <https://doi.org/10.1029/2018RG000619>
- Schilling, O. S., Cook, P. G., Grierson, P. F., Dogramaci, S., & Simmons, C. T. (2020). Controls on interactions between surface water, groundwater and riverine vegetation along intermittent rivers and ephemeral streams in arid regions. *Water Resources Research*, 57(2), e2020WR028429. <https://doi.org/10.1029/2020WR028429>
- Schilling, O. S., Doherty, J., Kinzelbach, W., Wang, H., Yang, P. N., & Brunner, P. (2014). Using tree ring data as a proxy for transpiration to reduce predictive uncertainty of a model simulating groundwater–surface water–vegetation interactions. *Journal of Hydrology*, 519, 2258–2271. <https://doi.org/10.1016/j.jhydrol.2014.08.063>
- Schilling, O. S., Gerber, C., Partington, D. J., Purtschert, R., Brennwald, M. S., Kipfer, R., et al. (2017). Advancing physically-based flow simulations of alluvial systems through observations of ^{222}Rn , $^3\text{H}/^3\text{He}$, atmospheric noble gases and the novel ^{37}Ar tracer method. *Water Resources Research*, 53(12), 10465–10490. <https://doi.org/10.1002/2017WR020754>
- Schilling, O. S., Irvine, D. J., Hendricks Franssen, H. J., & Brunner, P. (2017). Estimating the spatial extent of unsaturated zones in heterogeneous river-aquifer systems. *Water Resources Research*, 53(12), 10583–10602. <https://doi.org/10.1002/2017WR020409>
- Schilling, O. S., Parajuli, A., Tremblay Otis, C., Müller, T. U., Antolinez Quijano, W., Tremblay, Y., et al. (2021). Quantifying groundwater recharge dynamics and unsaturated zone processes in snow-dominated catchments via on-site dissolved gas analysis. *Water Resources Research*, 57(2), e2020WR028479. <https://doi.org/10.1029/2020WR028479>
- Schilling, O. S., Park, Y.-J., Therrien, R., & Nagare, R. M. (2019). Integrated surface and subsurface hydrological modeling with snowmelt and pore water freeze-thaw. *Ground Water*, 57(1), 63–74. <https://doi.org/10.1111/gwat.12841>
- Schilling, O. S., Partington, D. J., Doherty, J., Kipfer, R., Hunkeler, D., & Brunner, P. (2022). Supporting Information dataset DS1 for article “Buried paleo-channel detection with a groundwater model, tracer-based observations and spatially varying, preferred anisotropy pilot point calibration”.
- Schomburg, A., Schilling, O. S., Guenat, C., Schirmer, M., Brunner, P., & Le Bayon, R.-C. (2018). Topsoil structure stability in a restored floodplain: Impacts of fluctuating water levels, soil parameters and ecosystem engineers. *Science of the Total Environment*, 639, 1610–1622. <https://doi.org/10.1016/j.scitotenv.2018.05.120>
- Sebben, M. L., Werner, A. D., Liggett, J. E., Partington, D. J., & Simmons, C. T. (2013). On the testing of fully integrated surface-subsurface hydrological models. *Hydrological Processes*, 27(8), 1276–1285. <https://doi.org/10.1002/hyp.9630>
- Siegenthaler, C., & Huggenberger, P. (1993). Pleistocene Rhine gravel. Deposition of a braided river system with dominant pool preservation. In J. L. Best & C. S. Bristow (Eds.), *Braided rivers: Form, process and economic application* (Vol. 75, pp. 147–162). Geological Society.
- Siirila-Woodburn, E. R., & Maxwell, R. M. (2015). A heterogeneity model comparison of highly resolved statistically anisotropic aquifers. *Advances in Water Resources*, 75, 53–66. <https://doi.org/10.1016/j.advwatres.2014.10.011>
- Smakhtin, V. U. (2001). Low flow hydrology: A review. *Journal of Hydrology*, 240, 147–186. [https://doi.org/10.1016/S0022-1694\(00\)00340-1](https://doi.org/10.1016/S0022-1694(00)00340-1)

- Stonedahl, S. H., Harvey, J. W., & Packman, A. I. (2013). Interactions between hyporheic flow produced by stream meanders, bars, and dunes. *Water Resources Research*, 49, 5450–5461. <https://doi.org/10.1002/wrcr.20400>
- Sun, A. Y. (2018). Discovering state-parameter mappings in subsurface models using generative adversarial networks. *Geophysical Research Letters*, 45(20), 11137–11146. <https://doi.org/10.1029/2018GL080404>
- swisstopo. (2019). *Geological atlas of Switzerland (1:25,000): Map LK 1168*. Federal Office of Topography swisstopo. (Langnau i.E.).
- swisstopo. (2021). swissALTI3D. Retrieved from <http://www.cadastre.ch/internet/swisstopo/de/home/products/height/swissALTI3D/swissALTI3D.html>
- Tang, Q., Kurtz, W., Schilling, O. S., Brunner, P., Vereecken, H., & Hendricks Franssen, H.-J. (2017). The influence of riverbed heterogeneity patterns on river-aquifer exchange fluxes under different connection regimes. *Journal of Hydrology*, 554, 383–396. <https://doi.org/10.1016/j.jhydrol.2017.09.031>
- Tang, Q., Schilling, O. S., Kurtz, W., Brunner, P., Vereecken, H., & Hendricks Franssen, H.-J. (2018). Simulating flood induced riverbed transience using unmanned aerial vehicles, physically-based hydrological modelling and the ensemble Kalman filter. *Water Resources Research*, 54(11), 9342–9363. <https://doi.org/10.1029/2018WR023067>
- Therrien, R., & Sudicky, E. (1996). Three-dimensional analysis of variably-saturated flow and solute transport in discretely-fractured porous media. *Journal of Contaminant Hydrology*, 23, 1–44. [https://doi.org/10.1016/0169-7722\(95\)00088-7](https://doi.org/10.1016/0169-7722(95)00088-7)
- Thiros, N. E., Gardner, W. P., & Kuhlman, K. L. (2021). Utilizing environmental tracers to reduce groundwater flow and transport model parameter uncertainties. *Water Resources Research*, 57, e2020WR028235. <https://doi.org/10.1029/2020WR028235>
- Tikhonov, A. N., & Arsenin, V. Y. (1977). *Solutions of ill-posed problems*. Winston.
- Tonkin, M. J., & Doherty, J. (2005). A hybrid regularized inversion methodology for highly parameterized environmental models. *Water Resources Research*, 41. <https://doi.org/10.1029/2005WR003995>
- Wang, N., Chang, H., & Zhang, D. (2021). Deep-learning-based inverse modeling approaches: A subsurface flow example. *Journal of Geophysical Research: Solid Earth*, 126(2), e2020JB020549. <https://doi.org/10.1029/2020jb020549>
- White, J. T., Fienen, M. N., & Doherty, J. (2016). A python framework for environmental model uncertainty analysis. *Environmental Modelling & Software*, 85, 217–228. <https://doi.org/10.1016/j.envsoft.2016.08.017>
- Wohl, E. (2021). An integrative conceptualization of floodplain storage. *Reviews of Geophysics*, 59, e2020RG000724. <https://doi.org/10.1029/2020RG000724>
- Würsten, M. (1991). *GWB - Hydrogeologische untersuchungen aeschau: Schlussbericht (in German)*. Geotechnisches Institut.
- Zhan, C., Dai, Z., Soltanian, M. R., & Zhang, X. (2022). Stage-wise stochastic deep learning inversion framework for subsurface sedimentary structure identification. *Geophysical Research Letters*, 49(1), e2021GL095823. <https://doi.org/10.1029/2021GL095823>
- Zhu, Y., & Zabaras, N. (2018). Bayesian deep convolutional encoder-decoder networks for surrogate modeling and uncertainty quantification. *Journal of Computational Physics*, 366, 415–447. <https://doi.org/10.1016/j.jcp.2018.04.018>
- Zovi, F., Camporese, M., Hendricks Franssen, H.-J., Huisman, J. A., & Salandin, O. (2017). Identification of high-permeability subsurface structures with multiple point geostatistics and normal score ensemble Kalman filter. *Journal of Hydrology*, 548, 208–224. <https://doi.org/10.1016/j.jhydrol.2017.02.056>

References From the Supporting Information

- Ajami, H., McCabe, M. F., Evans, J. P., & Stisen, S. (2014). Assessing the impact of model spin-up on surface water-groundwater interactions using an integrated hydrologic model. *Water Resources Research*, 50, 2636–2656. <https://doi.org/10.1002/2013WR014258>
- Brunner, P., Simmons, C. T., Cook, P. G., & Therrien, R. (2010). Modeling surface water-groundwater interaction with MODFLOW: Some considerations. *Groundwater*, 48(2), 174–180. <https://doi.org/10.1111/j.1745-6584.2009.00644.x>
- de Marsily, G. (1978). *De l'identification des systems hydrogeologiques (Thèse de doctorat d'état)*. Ecole des Mines de Paris.
- Eriksson, M., & Siska, P. P. (2000). Understanding anisotropy computations. *Mathematical Geology*, 32(6), 683–700. <https://doi.org/10.1023/A:1007590322263>
- Everitt, B., & Hothorn, T. (2011). *An introduction to applied multivariate analysis with R*. Springer.
- James, G., Witten, D., Hastie, T., & Tibshirani, R. (2021). *An introduction to statistical learning with applications in R* (2nd ed.). Springer.
- Leskovec, J., Rajaraman, A., & Ullman, J. D. (2014). *Mining of massive datasets* (2nd ed.). Cambridge University Press.
- Merwade, V. M., Maidment, D. R., & Goff, J. A. (2006). Anisotropic considerations while interpolating river channel bathymetry. *Journal of Hydrology*, 331(3–4), 731–741. <https://doi.org/10.1016/j.jhydrol.2006.06.018>
- Moore, C., & Doherty, J. (2006). The cost of uniqueness in groundwater model calibration. *Advances in Water Resources*, 29, 605–623. <https://doi.org/10.1016/j.advwatres.2005.07.003>
- Seck, A., Welty, C., & Maxwell, R. M. (2015). Spin-up behavior and effects of initial conditions for an integrated hydrologic model. *Water Resources Research*, 51, 2188–2210. <https://doi.org/10.1002/2014WR016371>
- Severson, K. A., Molaro, M. C., & Braatz, R. (2017). Principal component analysis of process datasets with missing values. *Processes*, 5(38). <https://doi.org/10.3390/pr5030038>